






A case study on tundish fluid flow with electromagnetic stirring

Monika Zielińska^{1,2*} , Hongliang Yang³, Łukasz Madej² , Łukasz Malinowski¹ 

¹ Corporate Technology Center CTC, ABB sp. z o.o., Zeganska 1 st., 04-713 Warsaw, Poland.

² AGH University of Krakow, Department of Applied Computer Science and Modelling, Mickiewicza 30 av., 30-059 Krakow, Poland.

³ ABB AB/Metallurgy, Terminalvagen 24, Bldg 340, Vasteras 72159, Sweden.

Abstract

Tundish is a crucial component just before casting and plays a pivotal role in enhancing the cleanliness and overall homogeneity of the final steel composition. The paper deals with the development of an advanced Computational Fluid Dynamics (CFD) model, specifically focusing on the molten steel flow within the tundish to numerically support its further improvements. A noteworthy addition to the model is the consideration of an electromagnetic stirring device. This device significantly influences steel cleanliness and composition, thereby affecting the final properties of the formed metallic parts in subsequent processing stages.

The current investigation presents a comprehensive analysis of flow patterns and stirring energy distributions in relation to active and dead zones within the tundish. Through the developed coupled electromagnetic/fluid dynamic model, the paper demonstrates the feasibility of optimizing mixing processes to control the properties of the final product.

Keywords: Computational Fluid Dynamics, tundish fluid flow, electromagnetic stirring

1. Introduction

In the metallurgical industry, extensive research efforts are underway to achieve optimal product properties while minimizing production costs and environmental impact. The steel composition and microstructure substantially influence material behavior in subsequent metal processing stages, necessitating early process optimization in the production pipeline. Researchers are actively engaged in enhancing steel cleanliness, notably by reducing the amount of non-metallic inclusions to mitigate issues such as crack initiation in the final steel products. Effective inclusions removal is imperative for refining the steel production processes, and a considerable amount of research is devoted to this issue.

Zhang & Thomas (2003) comprehensively reviewed various sources of inclusions throughout the continuous

casting process. The mechanisms leading to the generation of inclusions in molten steel are intricate, influenced by factors such as the highly oxidizing atmosphere in the electrical arc furnace (EAF), reoxidation, and slag entrainment in subsequent production stages. Researchers concentrate on enhancing steel cleanliness, particularly in the ladle, tundish, and directly in the slab casting operations. Standard practices include the absorption of inclusions into the slag layer as presented by Reis et al. (2014), intensified removal processes through additional inert gas injection (Chang et al., 2018; Yang et al., 2019; Souza et al., 2020), the implementation of special channels with induction heating (Lei et al., 2019), or the incorporation of dedicated control devices, such as baffle walls or electromagnetic stirrers (EMS) applied by Zhang et al. (2000) and Li et al. (2020).

* Corresponding author: monika.zielinska@pl.abb.com

ORCID ID's: 0000-0001-7290-4330 (M. Zielińska), 0000-0003-1032-6963 (Ł. Madej), 0000-0002-1134-9473 (Ł. Malinowski)

© 2024 Author. This is an open access publication, which can be used, distributed and reproduced in any medium according to the Creative Commons CC-BY 4.0 License requiring that the original work has been properly cited.

The research on these topics relies heavily on mathematical or numerical modelling due to the challenges associated with measurements under actual production conditions. The Computational Fluid Dynamics (CFD) approach facilitates a comprehensive exploration of flow patterns and inclusion behaviors across various metallurgical equipment, ranging from the electrical arc furnace, through the ladle furnace and to the tundish. It also enables predictions of solidification phenomena arising from high-temperature gradients and low velocity, characteristics observed during the casting process.

Therefore, the main goal of this research is to develop a complex coupled electromagnetic/fluid dynamic model of the steel behavior in the tundish equipped with electromagnetic stirrers to understand how the stagnant velocity distribution areas and high-temperature gradients develop during the process. Material flow in the tundish is critical as it is the last production stage with fully liquid metal. As a result, the mixing process could be appropriately designed to increase the homogeneity

of the steel and avoid areas with stagnant flow or inhomogeneous temperature distribution. Both phenomena lead to severe problems related to the quality and clogging of the tundish nozzle. These issues are dangerous from a safety point of view and can lead to production faults, exposing the company to unexpected costs.

2. Methodology

The numerical investigations of the flow behavior inside the tundish were conducted with the commercial Ansys Fluent CFD software. The geometry of the tundish was recreated according to the specifications of the real industrial-scale device, as seen in Figure 1. Simulations were focused on the different computational scenarios within the tundish with additional control devices, namely: baffle walls, electromagnetic stirrers and stoppers (Fig. 2). The research aimed to compare the effectiveness of the mixing process in the case of baffle wall solutions and the EMS stirring method.

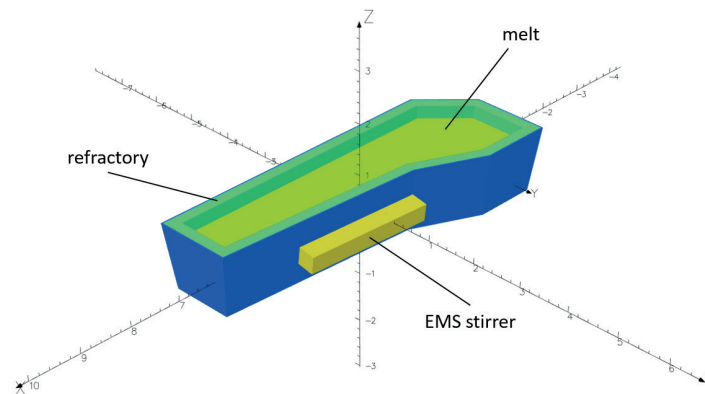


Fig. 1. The geometry of the tundish used in the numerical simulations with EMS location

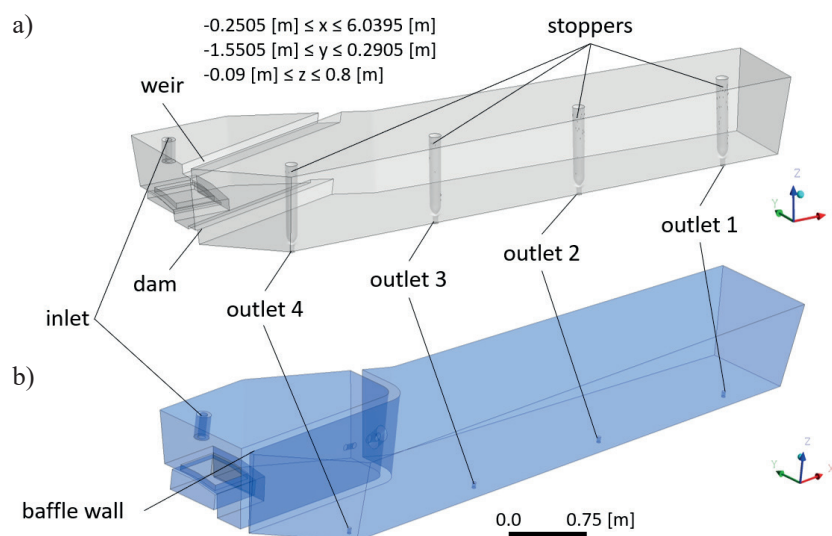


Fig. 2. The melt geometry within the tundish for the CFD numerical simulations with: a) stoppers; b) baffle wall

The steel properties used as input data are included in Table 1. The CFD simulation assumes a fully turbulent flow; therefore, the steel is modelled as an incompressible fluid, where properties do not depend on the temperature due to the relatively small temperature difference compared to the average temperature of entire melt inside the tundish.

Table 1. Steel properties

Density [kg/m ³]	7,200
Viscosity [kg/(m·s)]	0.0072
Thermal conductivity [W/(m·K)]	35
Heat capacity [J/(kg·K)]	692

An appropriate parametric study (Tab. 2) was designed to investigate the flow behaviour under different process setup scenarios in order to understand the influence of additional stirring mechanisms on the mixing process and optimise the power input to avoid energy losses. In the presented study, the 100% of EMS suggests that the electromagnetic stirrer works with its maximum power. This power can be controlled by the control of the current conditions applied to the stirrer and presented as a percentage value of the efficiency of the EMS system.

Table 2. Investigated process setup scenarios

Scenario no.	Description
1	without EMS, without baffle wall
2	with 100% of EMS, normal direction of stirring
3	with 100% of EMS, reversed direction of stirring
4	without EMS, with baffle wall
5	with 100% of EMS, without baffle wall, with stoppers
6	with 84% of EMS, without baffle wall, with stoppers
7	with 69% of EMS, without baffle wall, with stoppers
8	with 60% of EMS, without baffle wall, with stoppers
9	with 31% of EMS, without baffle wall, with stoppers

In the EMS-stirred tundish, the electromagnetic stirrer generates an electromagnetic field that acts on the molten steel. To capture this behavior in the developed CFD model, force distribution is calculated based on the Lorentz force assumption:

$$F = \sigma(E + U \times B) \times B \quad (1)$$

where: σ – electrical conductivity [S/m]; E – electric field [V/m]; U – velocity [m/s]; B – magnetic field [T].

The main assumption includes the harmonic behavior of the magnetic and electric fields in the following form:

$$F = \sigma(E_0 \times B) - \sigma \nabla \varnothing \times B + \sigma(U \times B) \times B \quad (2)$$

The first part of the equation is not dependent on the velocity and can be calculated for the assumption of the constant melt, but the second part depends on the motion of the melt and must be realized by the coupling between the two solvers, CFD and electromagnetic. The coupling is realized by the compensation of the force in each direction according to the travelling wave.

Finally, the electromagnetic stirring used to induce the steel flow is realized by the additional momentum source terms introduced into the momentum equation in the CFD approach. Forces from the electromagnetic stirring are compensated to include the impact of the velocity and mapped into the fluid computational domain. The following equation describes this dependence:

$$\vec{F} = \vec{F}_0 \left(1 - \frac{\vec{F}_0 \cdot \vec{V}}{2\tau f |\vec{F}_0|} \right) \quad (3)$$

where: \vec{F}_0 – stirring force calculated for stationary melt [N/m³]; \vec{F} – stirring force after compensation with moving melt [N/m³]; τ – pole pitch [m]; f – frequency [Hz]; \vec{V} – velocity of melt [m/s].

The exemplary force field mapping operation to include the effect of electromagnetic stirring in the tundish model is presented as a force density distribution along x , y and z in Figure 3.

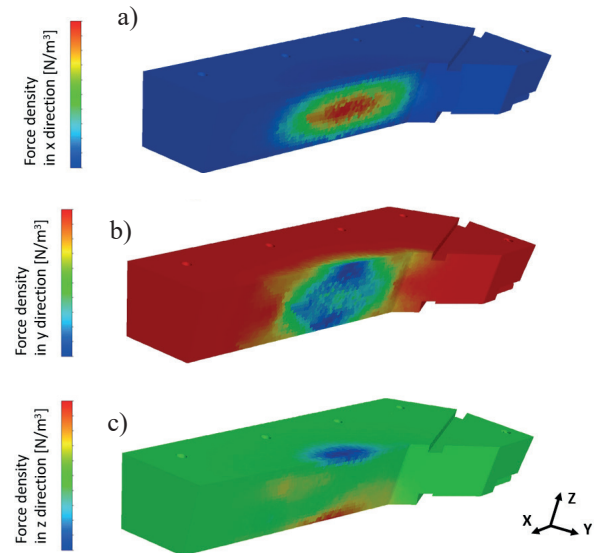


Fig. 3. Force densities field along 3 directions: a) x ; b) y ; c) z

The stirring energy value is calculated to characterise the flow inside the tundish based on the measurements of the turbulence dissipation rate presented by

Zielińska et al. (2023). The specified stirring energy is calculated according to the equation:

$$\dot{\epsilon} = \frac{\int_0^{\Omega} \epsilon d\Omega}{\int_0^{\Omega} d\Omega} \cdot 9.81 \cdot 1000 \left[\frac{\text{W}}{\text{t}} \right] \quad (4)$$

where: ϵ – turbulence dissipation rate [m^2/s^3]; Ω – volume of the melt [m^3].

Visualisation of the molten steel flow is realised by additional discrete phase particles available in the Discrete Phase Model (DPM). The particles act as tracers without influence on the melt flow and travel in time with the continuous phase, enabling the observation of the liquid steel's movement. The DPM visualisation allows the qualitative evaluation of the mixing process.

From the quantitative point of view, the effectiveness of the mixing process inside the tundish can be assessed based on the flow control theory presented by Sahai & Emi (1996) and combined or mixed models (Sahai & Emi, 2008). In this case, the focus is put on investigations of regions around plugs, well-mixed and dead zones to identify areas where improvement in the flow is needed. Three different regimes of the flow regions are described as:

– dead volume:

$$\frac{V_d}{V} = 1 - \frac{1}{N} \left(\frac{Q_{1a}}{Q_1} \times \theta_{1cut-off} + \frac{Q_{2a}}{Q_2} \times \theta_{2cut-off} + \dots + \frac{Q_{Na}}{Q_N} \times \theta_{Ncut-off} \right) \quad (5)$$

– plug volume:

$$\frac{V_p}{V} = \frac{1}{N} \left[\left(\frac{\theta_{1min} + \theta_{1peak}}{2} \right) + \left(\frac{\theta_{2min} + \theta_{2peak}}{2} \right) + \dots + \left(\frac{\theta_{Nmin} + \theta_{Npeak}}{2} \right) \right] \quad (6)$$

– well mixed volume:

$$\frac{V_m}{V} = 1 - \frac{V_p}{V} - \frac{V_d}{V} \quad (7)$$

where: V – volume [m^3]; N – number of strands [-]; Q – volumetric flow rate [m^3/s]; θ – dimensionless time [-] and subscripts correspond to the total flow rate (Q) per each strand, and flow rate by active region (Q_a).

In plug volume calculations, the θ_{min} is corresponding to the dimensionless time, when tracer occurred at the outlet and θ_{peak} is corresponding to the dimensionless time, when the peak of concentration at outlet is observed. The separate explanation is required for dead volume calculation due to the $\theta_{cut-off}$ parameter as a value calculated between $\theta = 0$ and $\theta = 2$:

$$\theta_{cut-off} = \frac{\sum_{i=0}^2 \theta_i c_i}{\sum_{i=0}^2 c_i} \quad (8)$$

where c is a dimensionless concentration of the tracer.

These models will be used to evaluate the mixing efficiency inside the tundish. The investigations are also based on the RTD (Residence Time Distribution) curves with pulse input of the tracer via the inlet (C-curve). The separate analysis also includes the constant input of the tracer via inlet (F-curve), which is characteristic of the intermixing process. This kind of process appears during the ladle changes with different steel grades.

The selected representative cases were calculated with an additional evaluation of the heat transfer inside the tundish. The developed numerical models with the illustration of the boundary conditions to reflect scenarios no. 1, 4 and 5 from Table 2 are presented in Figure 4.

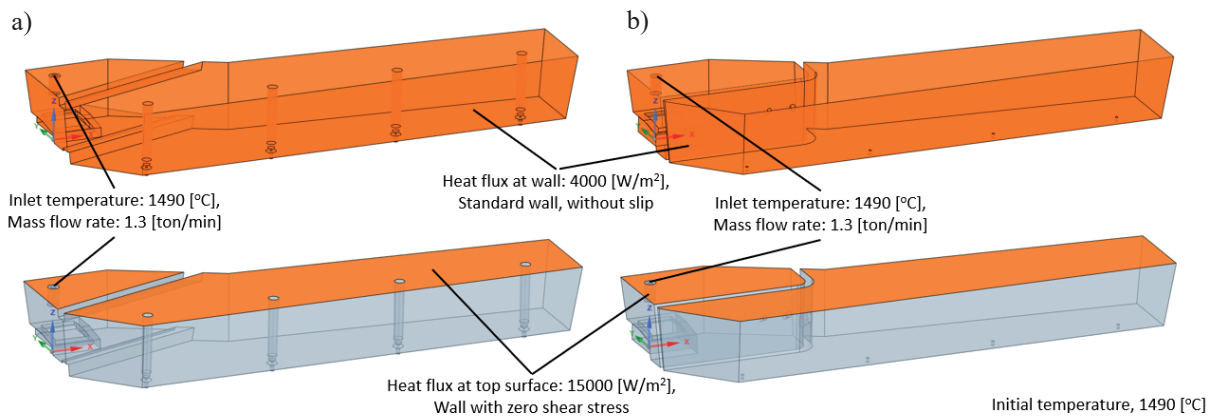


Fig. 4. Boundary conditions used for the simulation with heat transfer for: a) scenario no. 1 and no. 5; b) scenario no. 4

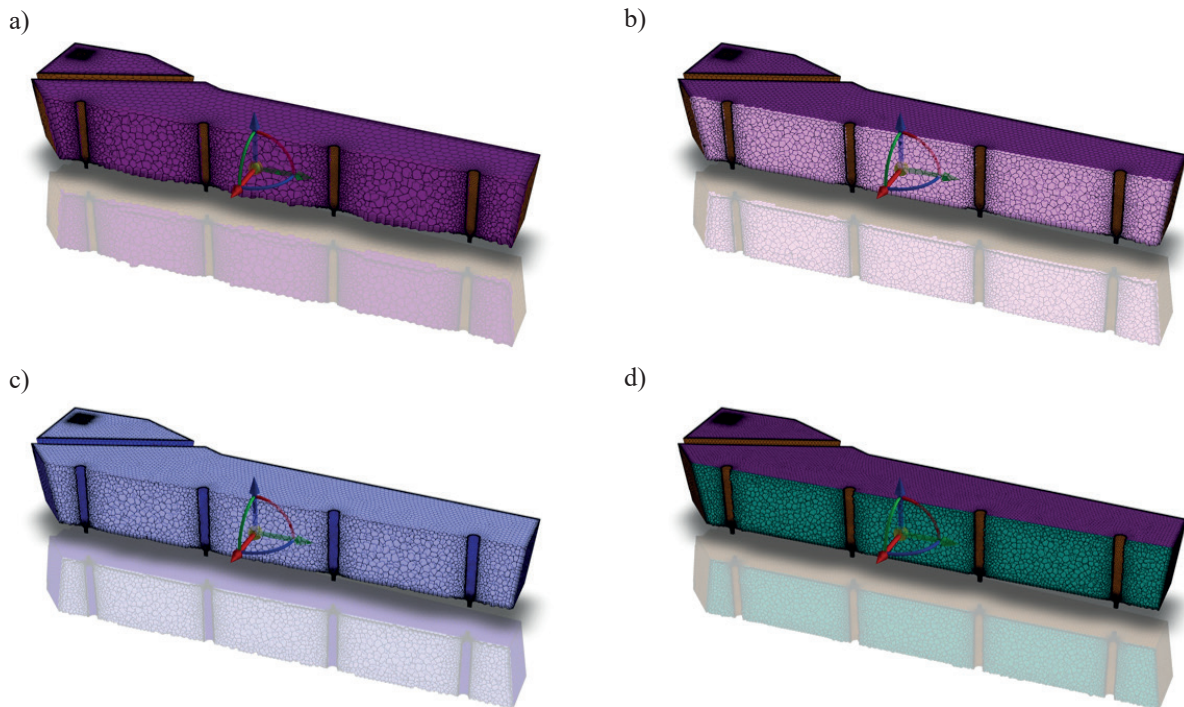


Fig. 5. Increasing mesh densities for the mesh sensitivity study of tundish: a) mesh 1 – 149,248 number of elements; b) mesh 2 – 176,298 number of elements; c) mesh 3 – 264,270 number of elements; d) mesh 4 – 592,041 number of elements

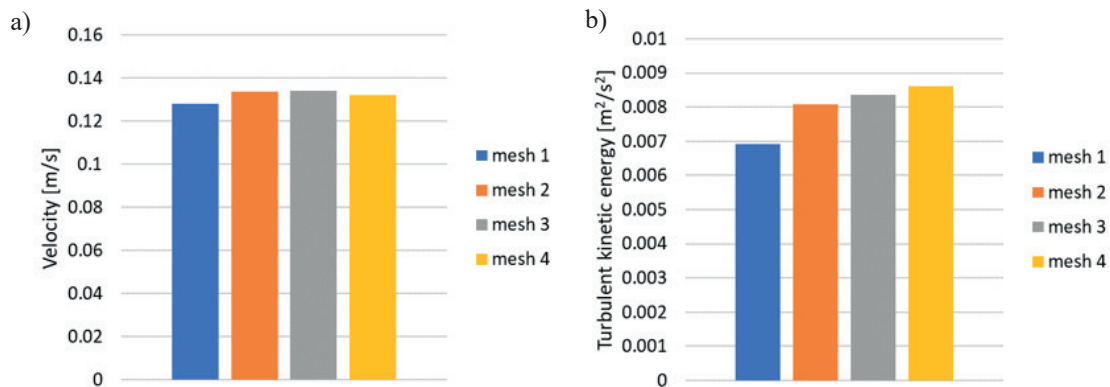


Fig. 6. The average value of the velocity (a) and turbulence (b) kinetic energy in the tundish domain obtained from the mesh sensitivity study

Before the main analysis, a mesh sensitivity study was conducted to ensure the quality of the results. Four different densities of the computational polyhedral mesh were prepared using the Ansys Fluent Meshing software (Fig. 5). Then, the steady state analysis was realised to compare the velocity (Fig. 6a) and turbulent kinetic energy (Fig. 6b) in the tundish domain.

The coarsest mesh provided an error between results (average value of the turbulent kinetic energy in the tundish domain) up to 17%. Between the rest of the results, the error is around 3%. The finest mesh, on the other hand, does not significantly increase the quality of results but extends the simulation time.

Therefore, based on the results presented above, the mesh density of mesh 3 (Fig. 5c) was selected for further investigation.

3. Results and discussion

The main simulations were performed according to settings from Table 2 to evaluate their influence on the velocity distribution and stirring effectiveness. The first comparison between the velocity and stirring energy distribution for 100%, 84%, 69%, 60% and 31% of EMS stirring force and for the case with stoppers is presented in Figure 7.

It is important to note that the occurrence of outlet clogging is a common phenomenon within the tundish, primarily influenced by the solidification of molten steel. This phenomenon is particularly related to the areas of dead zones and the sedimentation process, where various residues detach from the walls and obstruct the outlets. In contrast to the more intensive mixing process in the

ladle furnace, the relatively low stirring energy inside the tundish often contributes to this issue. Therefore, analysing the stirring energy near the outlets can enhance the design process and optimise the device's functionality. The comparison between the stirring energy distribution in the area of each outlet for cases with stoppers for 100% and 31% of EMS is presented in Figure 8.

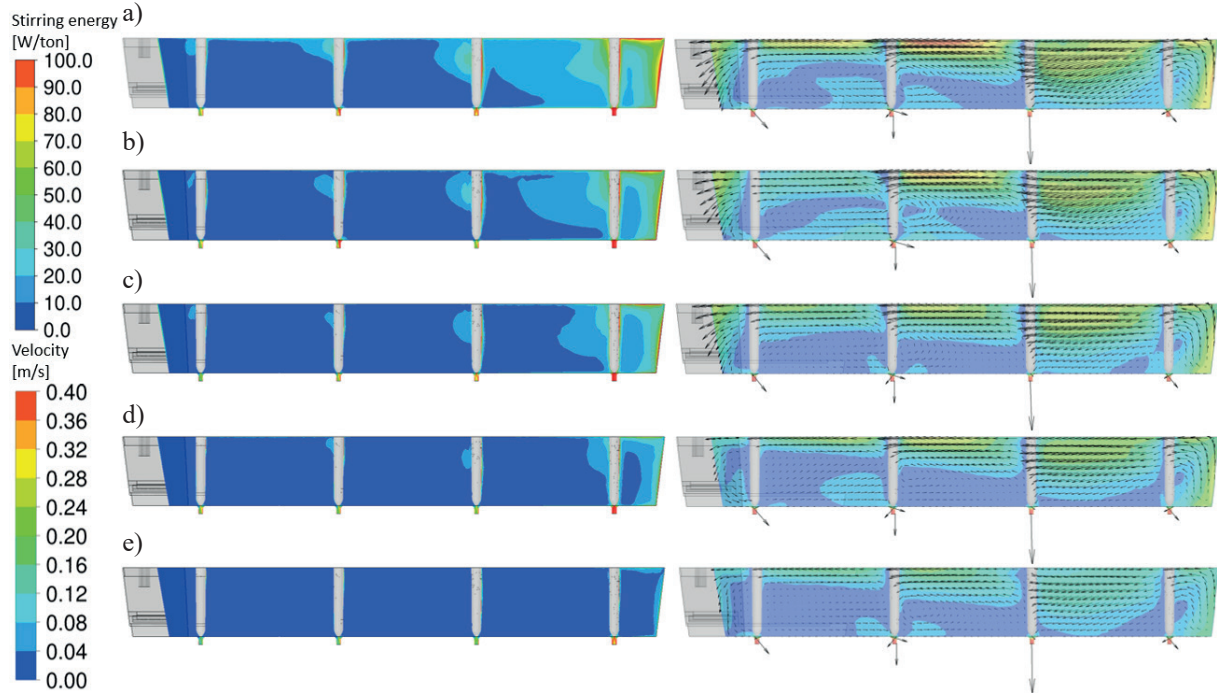


Fig. 7. Stirring energy (left) and velocity (right) distribution for different EMS force factors: a) 100% – case no. 5; b) 84% – case no. 6; c) 69% – case no. 7; d) 60% – case no. 8; e) 31% – case no. 9

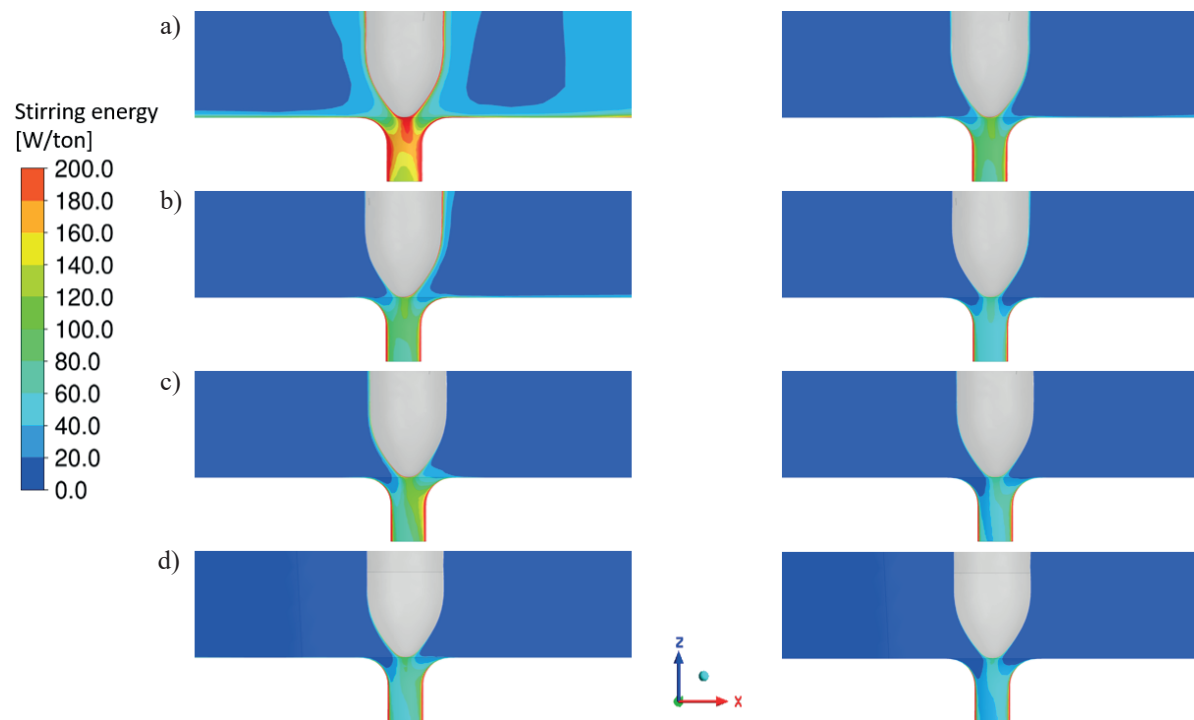


Fig. 8. Stirring energy distribution for case no. 5, 100% of EMS (left) and case no. 9, 31% of EMS (right) for different outlets: a) outlet 1; b) outlet 2; c) outlet 3; d) outlet 4

Based on Figure 8, stirring energy distribution close to outlet 3 has the most asymmetric character, and the gradients of the values are the highest. It can be assumed that the risk of clogging of that outlet is the highest in this case.

Another important investigation is the evaluation of the molten steel mixing intensity inside the tundish. This mixing can be easily visualised by the mentioned massless particles whose behaviour is dependent on

the steel flow in the tundish, as presented in Figure 9 and 10. The simulation model without additional control devices is used as a reference case and compared with the model with 100% of EMS. The investigation also included the reversed direction of the stirring to compare the behaviour of particles and the results with a common control device like a baffle wall with openings used to improve the liquid steel mixing process.

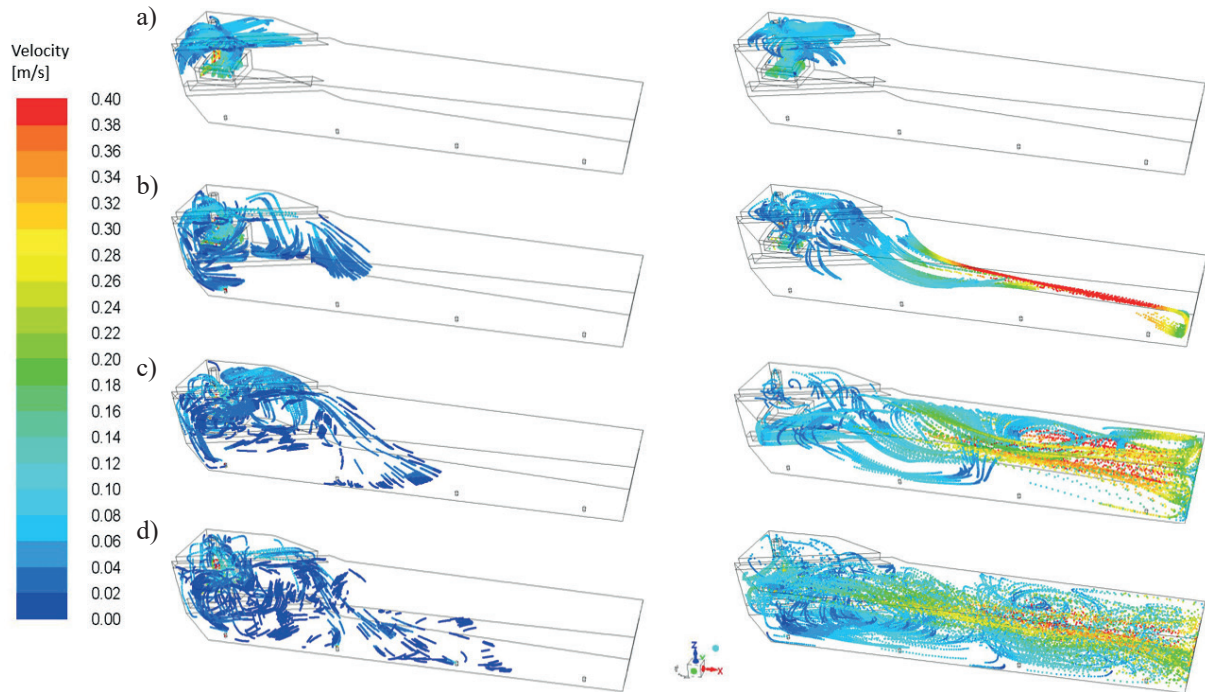


Fig. 9. Massless DPM tracers to visualise the mixing process for case no. 1 without EMS, without baffle wall (left) and for case no. 2 with 100% of EMS, the normal direction of stirring at: a) 20 s; b) 50 s; c) 100 s; d) 200 s

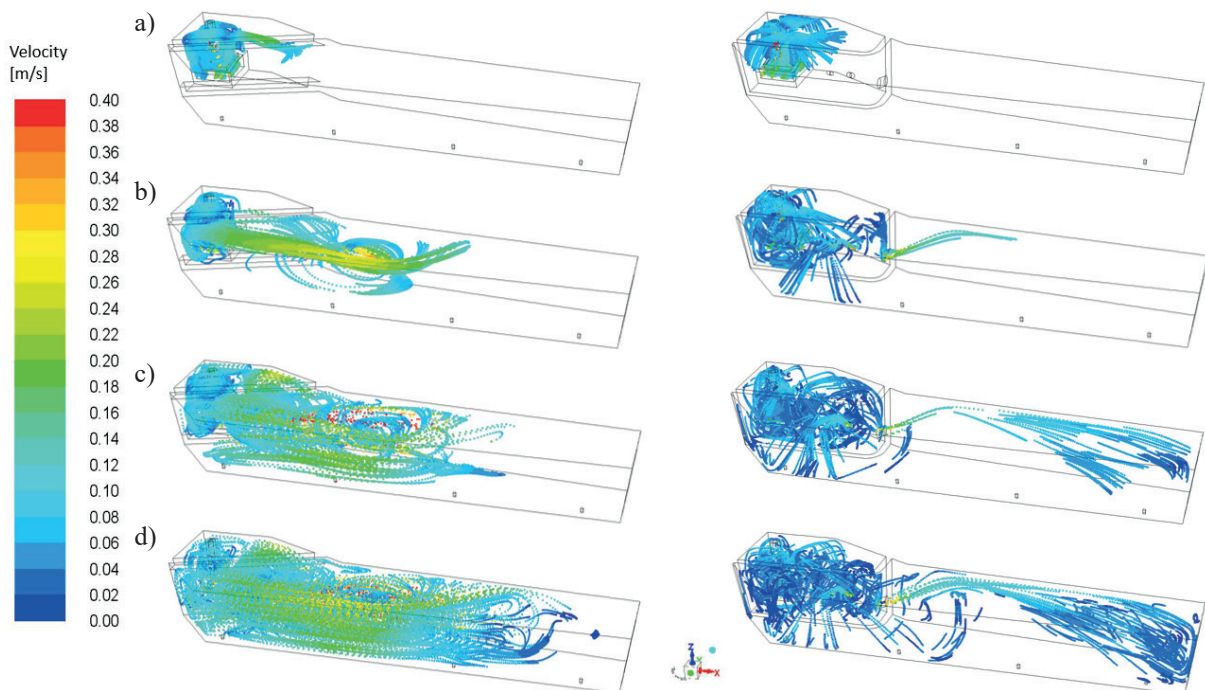


Fig. 10. Massless DPM tracers to visualise the mixing process for case no. 3 with 100% of EMS, reversed direction of stirring (left), and for case no. 4 without EMS, with baffle wall at: a) 20 s; b) 50 s; c) 100 s; d) 200 s

The comparison confirms that the best mixing is for the case with 100% EMS stirring. The results are much better than the baffle wall and indicate the high efficiency of homogenising velocities and temperatures. Obtained results also indicate an increase in the inclusion removal process, which is important to the steel’s quality. However, at the same time, it seems that the reversed direction of the EMS system does not provide satisfactory effects and thus this case will not be considered for further investigation.

To further prove the efficiency of the EMS stirring in a quantitative manner, the additional analysis of the RTD curves was conducted for three particular scenarios: 1 – without EMS and without baffle wall, 4 – without EMS but with baffle wall and 5 – with 100% of EMS, without baffle wall and with stoppers. The RTD curves, type C, where the concentration of the tracer was measured for each outlet, are presented in Figure 11. Moreover, the percentage values calculated separately for dead, plug and well-mixed volumes are shown in Table 3.

The dead, plug and well-mixed volumes were calculated according to the combined model (Sahai & Emi, 1996; Cendekia, 2018) for a multi-strand billet caster tundish. It is confirmed that the dead volume is the highest for cases without a flow control device, where the high plug volume is also observed. The highest well-mixed volume and the smallest plug volume are observed in the case of EMS stirring. Moreover, the character of the curves is very similar to the ideal mixing curves. Based on the analysis of these curves, the combined method seems to not fit well for EMS systems due to the similarity of the curves to the ideal mixing curve but still quite a large value of the dead zone volume. From the combined model, it seems that the case with the existing baffle wall should provide the best mixing, which seems to be not true based on the observations of the behavior of the tracer in the numerical model and qualitative comparison between the simulation results presented in Figure 12.

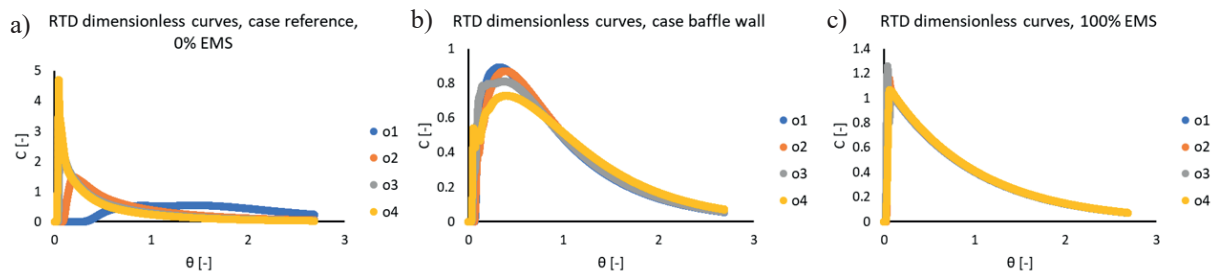


Fig. 11. C-curves for: a) reference case without EMS, without baffle wall; b) case with baffle wall; c) case with 100% of EMS and without baffle wall, with stoppers

Table 3. Percentage of the dead, plug and well-mixed volumes in the tundish

Scenario	Dead volume [%]	Plug volume [%]	Well-mixed volume [%]
Without EMS, without baffle wall	36.6	14.1	49.3
Without EMS, with baffle wall	26.4	13.2	60.5
With 100% of EMS, without baffle wall, with stoppers	34.6	2.2	63.3

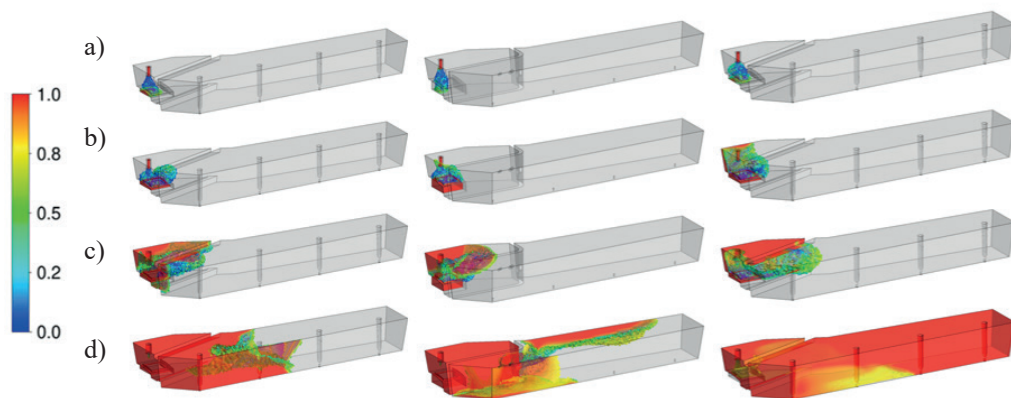


Fig. 12. Dimensionless concentration of a tracer obtained from CFD simulation for case without flow control device (left), for case with standard, existing baffle wall (middle) and for case with EMS system (right) for: a) tracer start injection time; b) observations after 5 s; c) observations after 20 s; d) observations after 120 s

The complementation of the research is a calculation of the intermixing process, which is shown based on the F-curves. The research was conducted for the same cases as for the C-curve analysis above. A comparison of the results is presented in Figure 13.

The best similarity between curves for each outlet is for the case with the EMS system, which confirms the best homogenisation of the steel structure in time and the same properties of the steel for each strand after steel grade changes.

The final analysis to confirm the effectiveness of the EMS system is based on the simplified steady-state simulation of the heat transfer inside the tundish during the process. The temperature distribution (Fig. 14) and evolution of the homogenisation process are gathered in Figure 15.

The EMS system was applied in different current scenarios, but the results suggest that even a small power input provides better temperature distribution and homogeneity in the whole bath and at each outlet. The most significant difference in the temperature distribution is for the case without any flow control device, where the lowest value of the temperature is presented. The temperature differences are also observed in the case with the baffle wall, close to outlet number 4. That suggests that the risk of the local solidification and then clogging of outlets is high. Finally, it is clear that the EMS stirrer ensures great temperature homogenisation in the whole volume of the tundish and no occurrence of dead zones.

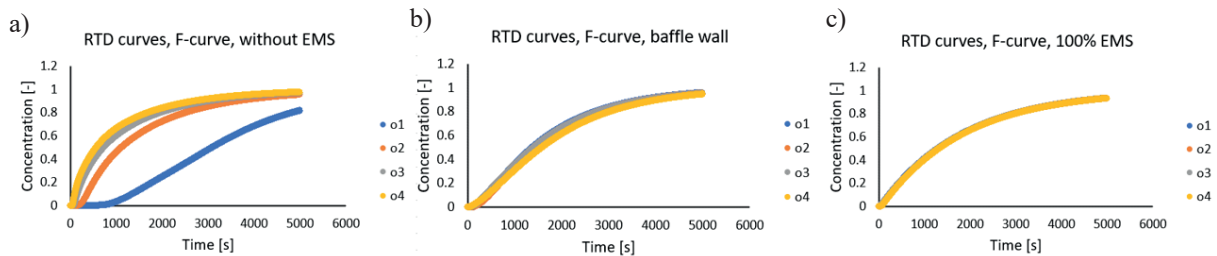


Fig. 13. F-curves for: a) reference case without EMS, without baffle wall; b) case with baffle wall; c) case with 100% of EMS and without baffle wall, with stoppers

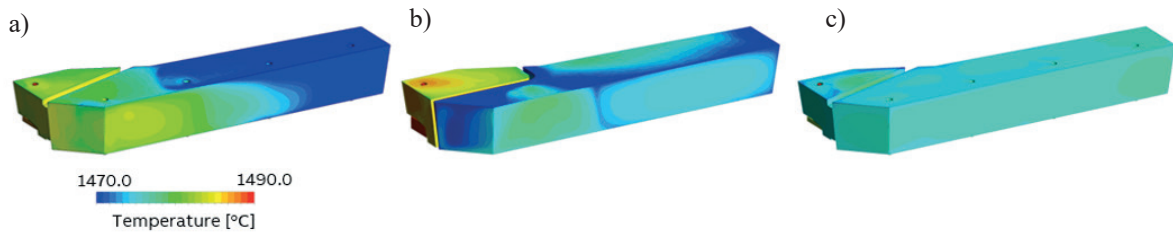


Fig. 14. Temperature distribution for case: a) 1; b) 4; c) 5

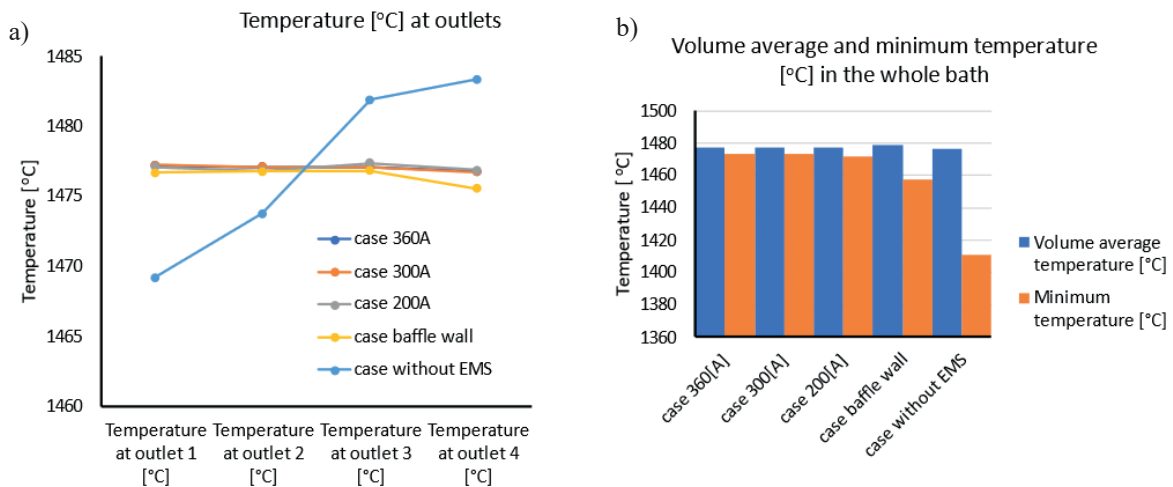


Fig. 15. Temperature in the form of: a) surface-averaged values measured at each outlet; b) volume average and minimum values measured in the whole bath of tundish

4. Conclusions

Based on the presented research, the following conclusions can be formulated:

- CFD simulations enable us to understand the issues in the steelmaking industry and optimize the continuous casting process to improve the effectiveness of the work of metallurgical devices.
- The electromagnetic stirrers can greatly improve the molten steel flow and temperature distribution inside the tundish. In this case, a relatively low power input significantly improves the effectiveness of the mixing. As a result, the homogenization of the structure and purity of the steel is improved. At the same time, the agglomeration of inclusions into the slag will occur due to the prevention of the dead zones. As a result, areas with stagnant flow influencing the velocity and temperature are minimized, which is confirmed by the similarity of the

RTD curve to the ideal mixing curve. All those aspects directly influence the final product's quality.

- The EMS stirring also prevents uncontrolled solidification and sedimentation, which is dangerous from a safety point of view due to the risk of clogging and faults in the production line. This aspect is directly related to excellent temperature homogenization and lack of regions with low temperatures where the solidification process can start.
- The above-mentioned conclusions indicate that the electromagnetic stirrers can precisely control the structure of the molten steel.

Acknowledgments

The research was conducted within the scope of an industrial doctorate project co-financed by the Ministry of Science and Education.

References

- Cendekia, B. B. (2018). *The Effect of Electromagnetic Stirring and Flow Control Devices on Flow Characteristics in Eight-strand Tundish* [Master's thesis, KTH Royal Institute of Technology, School of Industrial Engineering and Management]. <https://kth.diva-portal.org/smash/get/diva2:1229627/FULLTEXT01.pdf>.
- Chang, S., Cao, X., Zou, Z., Isac, M., & Guthrie, R. I. L. (2018). Micro-bubble formation under non-wetting conditions in a full-scale water model of a ladle shroud/tundish system. *ISIJ International*, 58(1), 60–67. <https://doi.org/10.2355/isijinternational.ISIJINT-2017-390>.
- Lei, H., Yang, B., Bi, Q., Xiao, Y., Chen, S., & Ding, Ch. (2019). Numerical simulation of collision-coalescence and removal of inclusion in tundish with channel type induction heating. *ISIJ International*, 59(10), 1811–1819. <https://doi.org/10.2355/isijinternational.ISIJINT-2019-118>.
- Li, B., Lu, H., Zhong, Y., Rens, Z., & Lei, Z. (2020). Numerical simulation for the influence of EMS position on fluid flow and inclusion removal in a slab continuous casting mold. *ISIJ International*, 60(6), 1204–1212. <https://doi.org/10.2355/isijinternational.ISIJINT-2019-666>.
- Reis, B. H., Bielefeldt, W. V., & Vilela, A. C. F. (2014). Efficiency of inclusion absorption by slags during secondary refining of steel. *ISIJ International*, 54(7), 1584–1591. <https://doi.org/10.2355/isijinternational.54.1584>.
- Sahai, Y., & Emi, T. (1996). Melt flow characterisation in continuous casting tundishes. *ISIJ International*, 36(6), 667–672. <https://doi.org/10.2355/isijinternational.36.667>.
- Sahai, Y., & Emi, T. (2008). *Tundish Technology for Clean Steel Production*. World Scientific Publishing. <https://doi.org/10.1142/6426>.
- Souza, G. M., Mendonça, A. F. G., & Tavares, R. P. (2020). Physical and mathematical modeling of inclusion behavior in a tundish with gas curtain. *REM – International Engineering Journal*, 73(4), 531–538. <https://doi.org/10.1590/0370-44672020730010>.
- Yang, H., Vanka, S. P., & Thomas, B. G. (2019). Mathematical modeling of multiphase flow in steel continuous casting. *ISIJ International*, 59(6), 956–972. <https://doi.org/10.2355/isijinternational.ISIJINT-2018-743>.
- Zhang, L., & Thomas, B. G. (2003). Inclusions in continuous casting of steel. *XXIV National Steelmaking Symposium, Morelia, Mich, Mexico, 26–28 Nov. 2003* (pp. 138–183). https://www.researchgate.net/publication/228857732_Inclusions_in_continuous_casting_of_steel.
- Zhang, L., Taniguchi, S., & Cai, K. (2000). Fluid flow and inclusion removal in continuous casting tundish. *Metallurgical and Materials Transactions B*, 31(2), 253–266. <https://doi.org/10.1007/s11663-000-0044-9>.
- Zielińska, M., Yang, H., Madej, Ł., & Malinowski, Ł. (2023). Influence of electromagnetic field on stirring energy in selected metallurgical equipment. *Steel Research International*, 95(3), 2300534. <https://doi.org/10.1002/srin.202300534>.